

Fig. 2. (a) Output buffer and dummy buffer (b) simulated equivalent loading capacitances and capacitive loading variation due to buffer.

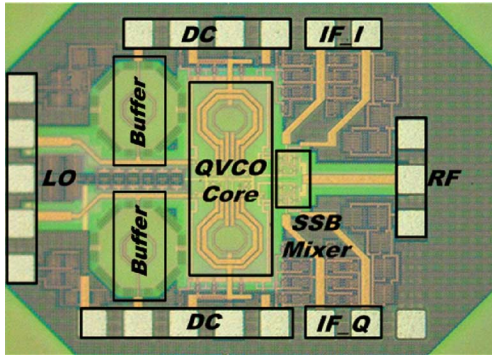


Fig. 3. Die photo of the QVCO using microwave trifilar transformers.

suitable coupling strengths, instead of different turn ratios. The gate-to-drain coupling should be high enough to assure of a good inductor quality factor and overall phase noise. However, the gate/drain-to-source coupling provides a mutual coupling between I- and Q-VCOs and suffers from trade-offs between phase error and phase noise properties. Thus, the source line should be designed slightly away from the gate/drain lines to reduce the coupling strength. After fine-tuning, the trifilar transformer has an outer diameter of $140 \mu\text{m}$ with the metal thickness of $3.3 \mu\text{m}$. The line widths ($W_1/W_2/W_3$) are $9/12/3 \mu\text{m}$ and line spacing (S_1/S_2) are $2/7 \mu\text{m}$, respectively, where W_1-W_3 and S_1-S_2 are indicated in Fig. 1(b). The corresponding coupling coefficients k_{gd} , k_{ds} , and k_{gs} are 0.67, 0.35, and 0.3, respectively.

To fairly compare the two different layouts (the conventional 2:1:1 and newly proposed 1:1:1 types), the same oscillation frequency of 30 GHz and similar frequency tuning range are designed. As a result, the equivalent tank parallel resistance [$R_p \approx (1 + Q^2)R_s \propto Q^2$] of the QVCO (at resonance) using the 1:1:1 layout is around 1.6 times higher than that using the 2:1:1 layout. The corresponding simulated phase noise properties are indicated in Fig. 4(b) in Section III. The phase noise is then improved by around 4 dB at 1 MHz offset frequency. Note that, the chosen 2:1:1 trifilar transformer for comparison has the coupling coefficients k_{gd} , k_{ds} , and k_{gs} of 0.5, 0.5, and 0.25, respectively. Different turn ratios of the two cases result in different optimal design of coupling strengths.

A common-source (CS) buffer amplifier with an inductive load is used here to maintain the high-frequency response. For area saving, only one CS amplifier is employed in each I/Q-VCO, say I+ and Q+, as shown in Fig. 2(a). However,

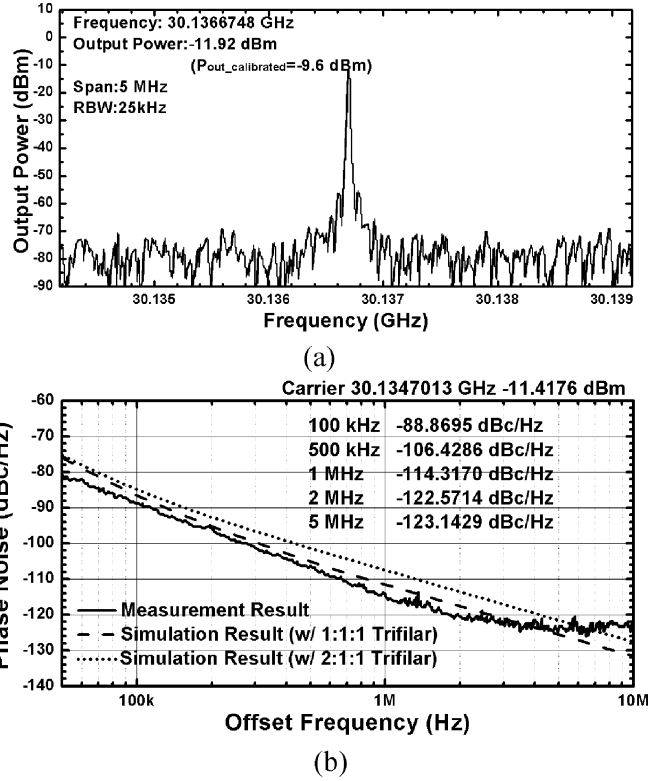


Fig. 4. (a) Output signal spectrum and (b) phase noise spectrum of the QVCO using microwave trifilar transformers.

this placement may cause significant signal imbalance. Thus, a dummy transistor with an open drain node is employed at the other port of each VCO, *i.e.*, I- and Q-. The simulated load capacitance of both CS buffer and open-loaded dummy are shown in Fig. 2(b). After fine-tuning, at a target-oscillation band of around 20 to 30 GHz, the capacitance loading is minimized. Note that, parasitic capacitance matching can be further improved by connecting the drain bias of the dummy transistor to V_{D2} at the cost of additional power consumption.

A standard single-sideband upconversion passive mixer is implemented to fairly measure I/Q phase error of the QVCO [1] to avoid the measurement inaccuracy resulting from amplitude/phase mismatches in wires and connectors at high frequencies. Besides, assuming the sideband rejection (SBR) in an upconversion is totally dominated by the quadrature phase error (ϕ) of the LO oscillator

$$SBR = -20 \log \left| \tan \left(\frac{\phi}{2} \right) \right|. \quad (1)$$

Once the SBR is measured, the equivalent worst-case phase error can be obtained by (1).

III. MEASUREMENT RESULTS

Fig. 3 shows the die photo of the QVCO utilizing a pair of microwave trifilar transformers. The die size is $1.1 \times 0.8 \text{ mm}^2$ while the QVCO core only occupies $180 \times 450 \mu\text{m}^2$. The supply voltage of the VCO core is 0.6 V with the core current consumption of 13 mA, while each CS buffer consumes 1.6 mA from a 1.2 V supply. Both the output signal spectrum and the phase noise spectrum are measured by Agilent E5052A signal

TABLE I
PERFORMANCE COMPARISON

Reference	Supply (V)	Frequency Range (GHz)	Power Consumption (mW)	Sideband Rejection (dB)	Phase Error	Phase Noise (at 1 MHz offset)	FOM ^b (dBc/Hz)	FOM _T ^c (dBc/Hz)	Technology
[5]	1	14.8-17.6	5	38	1.4° ^a	-110 dBc/Hz	-187.6	-192.4	0.18- μ m CMOS
[6]	1.2	5.65-5.9	8.64	37.7	1.5° ^a	-125.8 dBc/Hz	-191.6	-184.3	0.35- μ m SiGe HBT
[8]	1.45	4.94-5.22	8.7	N.R.	0.65°	-124.6 dBc/Hz	-189.4	-184.2	0.18- μ m CMOS
[9]	1.4	5.3-5.44	11.2	N.R.	\sim 5°	-119 dBc/Hz	-183	-171.3	0.18- μ m CMOS
[10]	3	22.07-22.9	187.5	N.R.	N.R.	-121.2 dBc/Hz	-185.6	-177	InGaP/GaAs HBT
This Work	0.6	26.8-30.3	7.8	41.6	0.95° ^a	-114.3 dBc/Hz	-195	-196.7	0.13- μ m CMOS

^a calculated from Eqn. (1).

^b FOM = $PN - 20\log(f_0/\Delta f) + 10\log(P_{DC}/1\text{mW})$, where PN = phase noise, f_0 = center frequency, Δf = offset frequency, and P_{DC} = VCO core power consumption.

^c FOM_T = $PN - 20\log(f_0/\Delta f) - 20\log(TP/10\%) + 10\log(P_{DC}/1\text{mW})$, where TP = tuning percentage.

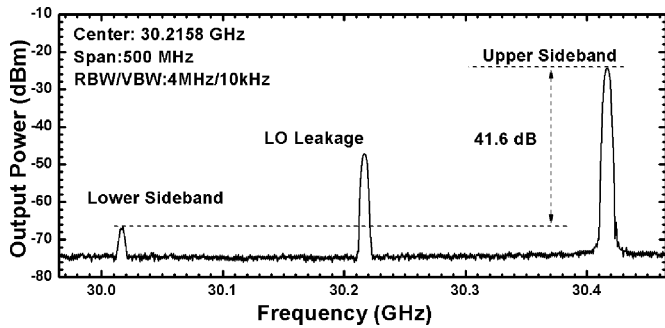


Fig. 5. Output spectrum at RF port of the single-sideband upconverter with a 41.6 dB sideband rejection.

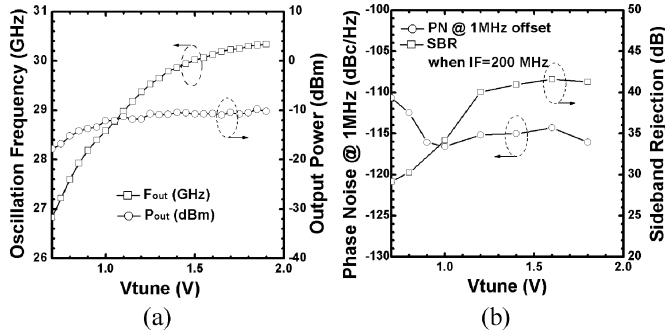


Fig. 6. (a) Oscillation frequency and output power (b) phase noise at 1 MHz offset and sideband rejection of the proposed QVCO.

source analyzer with Agilent N5507A microwave downconverter (1.5 to 26.5 GHz) and Agilent 11970A (26.5 to 40 GHz) waveguide harmonic mixer modules. Fig. 4(a) shows the output signal spectrum around 30 GHz while the phase noise of the proposed QVCO is -114.3 dBc/Hz at 1 MHz offset frequency, as shown in Fig. 4(b). Note that, the difference between the simulated and measured data may result from the inaccuracy of the CMOS device flicker noise model. Fig. 5 shows the output frequency spectrum measured by Agilent E4448A spectrum analyzer at the RF port of the upconverter with a 41.6 dB sideband rejection (SBR) while the IF frequency is 200 MHz. The differential-quadrature IF signals are generated from off-chip passive quadrature hybrid (SMC DQK-705; 150–300 MHz) and differential transformer baluns (Tyco Electronics H-9; 2–2000 MHz). Besides, phase shifters are also employed to compensate the phase error of the balun, hybrid, and wire connections to probes. As a result, a 41.6 dB SBR is equivalent to a phase error of approximately 0.95° calculated from (1). The LO leakage results from slightly unbalanced buffer loading,

phase error in passive IF balun, and also the device mismatches in the QVCO and the upconversion mixer.

The oscillation power and frequency of the proposed QVCO with respect to the tuning voltage are shown in Fig. 6(a). The output power of the QVCO stays around -10 dBm at frequency ranging from 28.5 to 30.3 GHz and falls to -18 dBm at 26.8 GHz. Note that, the simulated output power of the VCO core (without buffers) is -3 dBm. Besides, the phase noise at 1 MHz offset frequency and the SBR with respect to the tuning voltage are shown in Fig. 6(b). As a result, the phase noise at 1 MHz offset frequency is at most -115 dBc/Hz while the maximum SBR is 41.6 dB, and at least 29 dB covering the whole oscillation frequency band. The performance benchmark of the proposed QVCO and the state-of-the-art QVCOs [5], [6], [8]–[10] are summarized in Table I. Thus, both the FOM and FOM_T of the proposed QVCO are better than that of other QVCOs.

IV. CONCLUSION

A pair of 1:1:1 trifilar transformers in the proposed 30 GHz QVCO are used for high-frequency, low-area, and low-voltage operations. The 30 GHz QVCO achieves -195 dBc/Hz FOM and maximum SBR of 41.6 dB with the VCO core area of only $180 \times 450 \mu\text{m}^2$.

REFERENCES

- [1] A. Rofougaran, J. Rael, M. Rofougaran, and A. A. Abidi, "A 900 MHz CMOS LC-oscillator with quadrature outputs," in *IEEE ISSCC Dig. Tech. Papers*, 1996, pp. 391–393.
- [2] P. Andreani, A. Bonfanti, L. Romano, and C. Samori, "Analysis and design of a 1.8 GHz CMOS LC quadrature VCO," *IEEE J. Solid-State Circuits*, vol. 37, no. 12, pp. 1738–1747, Dec. 2002.
- [3] D. Baek, T. Song, E. Yoon, and S. Hong, "8 GHz CMOS quadrature VCO using transformer-based LC-based LC tank," *IEEE Microw. Wireless Compon. Lett.*, vol. 13, no. 10, pp. 446–448, Oct. 2003.
- [4] Y. Zhang, P. Upadhyaya, L. Peng, D. Rector, and D. Heo, "Analysis of resonator phase shift for two series LC quadrature VCOs," *Electron. Lett.*, vol. 44, no. 1, pp. 26–27, Jan. 2008.
- [5] A. W. L. Ng and H. C. Luong, "A 1-V 17 GHz 5-mW quadrature VCO based on transformer coupling," *IEEE J. Solid-State Circuits*, vol. 42, no. 9, pp. 1933–1941, Sep. 2007.
- [6] J.-S. Syu, C. C. Meng, and G.-W. Huang, "SiGe HBT quadrature VCO utilizing trifilar transformers," in *IEEE ASSCC Dig.*, 2008, pp. 465–468.
- [7] J. Yang, C.-Y. Kim, D.-W. Kim, and S. Hong, "Design of a 24 GHz CMOS VCO with an asymmetric-width transformer," *IEEE Trans. Circuits Syst. II*, vol. 57, no. 3, pp. 173–177, Mar. 2010.
- [8] S.-L. Jang, C.-C. Shih, C.-C. Liu, and M.-H. Juang, "A 0.18 μm CMOS quadrature VCO using the quadruple push-push technique," *IEEE Microw. Wireless Compon. Lett.*, vol. 20, no. 6, pp. 343–345, Jun. 2010.
- [9] I.-S. Shen, T.-C. Huang, and C. F. Jou, "A low phase noise quadrature VCO using symmetrical tail current-shaping technique," *IEEE Microw. Wireless Compon. Lett.*, vol. 20, no. 7, pp. 399–401, Jul. 2010.
- [10] C.-Y. Kim, J. Yang, D.-W. Kim, and S. Hong, "A K-band quadrature VCO based on asymmetric coupled transmission lines," in *IEEE MTT-S Int. Dig.*, Jun. 2008, pp. 363–366.